ORIGINAL RESEARCH **Open access**

AI-Controlled Energy Management in PV Systems Using Fuzzy-Neural Network Techniques

Emily Carter[1], James Martinez[2*], David Kim[3]

Abstract

Sustainable power networks, including photovoltaic (PV) systems, have gained substantial relevance due to growing concerns about climate change and the critical need to reduce greenhouse gas emissions. The deployment of static converters within solar energy configurations modifies the current, leading to reactive power consumption. To control active and reactive power, a proportional-integral controller is applied, while energy storage units improve power quality by maintaining voltage and current, directly influencing steady-state error. Incorporating artificial intelligence (AI) is essential to maximize the generation capacity of PV installations across diverse weather scenarios, given that traditional controllers fail to optimize solar energy yields adequately. Nonetheless, environmental changes can still impact PV system performance. This paper introduces an innovative strategy to improve the input efficiency of solar PV systems via adaptive neuro-fuzzy inference systems (ANFIS). A controller grounded in fuzzy neural inference was constructed and evaluated from both energy production and load demand viewpoints. This research investigates how artificial intelligence supports uninterrupted power delivery to consumers through battery storage, underscoring its role in load management. Furthermore, the outcomes revealed encouraging potential for power regulation and control.

Keywords Administrative management, Artificial Intelligence (AI), Photovoltaic array, PV framework, Fuzzy-neural network regulation, Power control

*Correspondence:
James Martinez
james.martinez@berkeley.edu
[1] Department of Artificial Intelligence for Microgrid Systems, Faculty of Electrical Engineering, Massachusetts Institute of Technology, Cambridge, United States
[2] Department of Intelligent Energy Analytics and Smart Grids, College of Engineering, University of California, Berkeley, Berkeley, United States
[3] Department of AI-Based Distributed Energy Resources, Faculty of Engineering, Stanford University, Stanford, United States

Introduction

Global attention toward renewable energy sources stems from multiple drivers. First, numerous industrialized nations experience elevated pollution levels, motivating public opposition against the construction of traditional thermal power facilities. Consequently, implementing renewable energy installations as substitutes for conventional infrastructure presents the primary remedy to this challenge. Second, certain nations rely heavily on nuclear facilities for electrical power. Following multiple nuclear catastrophes in Japan and Russia, widespread social opposition emerged against this form of power generation [1]. This led to the progressive substitution of nuclear stations with clean energy alternatives, a transition pioneered by countries like Germany. Third, several territories lack sufficient domestic fossil fuel reserves, such as coal and natural gas, which are vital for industrial power and economic progression [2]. As a result, nations without petroleum reserves began developing their local green resources, spanning solar, wind, tidal, and biomass alternatives [3]. Combined configurations utilizing renewable energy sources (RES), such as integrated solar and wind installations, provide innovative alternatives for isolated, off-grid regions while substantially lowering greenhouse gas outputs [4].

This is an open access article distributed under the terms of the Creative Commons Attribution-NonCommercial-ShareAlike 4.0 International License (CC BY-NC-SA 4.0), which permits non-commercial use, distribution, reproduction, and adaptation in any medium or format, provided that appropriate credit is given to the original author(s) and source, a link to the license is provided, and any changes made are indicated. Adapted material must be distributed under the same license.

© 2024 The Author(s). | Published by Institute of Smart Energy Systems Press

Although properly combined energy options leverage complementary strengths to offset individual limitations, they may yield inconsistent power delivery due to volatile meteorological and climate shifts [5]. Consequently, to address the challenge of creating reliable standalone generation setups, energy developers are turning toward hybrid systems that integrate traditional generators alongside renewable resources. These configurations are extensively deployed for electrification in isolated communities [6]. A key challenge in hybrid generation architectures involves sizing optimization for off-grid wind and photovoltaic components [7]. Establishing the ideal count and category of units is achieved by minimizing the cumulative system expense, thereby ensuring economic viability and environmental sustainability [8]. Multiple methodologies have been introduced to optimize sizing within hybrid electricity systems. Integrated wind and solar systems are generally structured for standalone operations or grid interaction. To satisfy the yearly load demand, an ideal configuration of wind and solar generators combined with an energy storage battery is typically utilized [9]. Based on various power demand patterns, comparative viability assessments have evaluated green energy utilization against erecting transmission infrastructure from the closest substation to deliver electricity to wind-solar grid networks [10]. The most efficient quantity and specification of units are established by minimizing the aggregate system cost across a 20-year horizon while satisfying load demands [11]. Crucially, the cost function optimization utilizes specialized algorithms capable of identifying near-optimal or highly favorable configurations via straightforward computational procedures [12]. Regarding alternative dimensioning algorithms for comparable hybrid setups, particle swarm optimization (PSO) has been selected for its rapid processing and efficient convergence behavior, demonstrating superior performance relative to standard genetic algorithms documented in previous research [13]. Alternatively, the simulated annealing method is effectively deployed to minimize the total investment of hybrid configurations, yielding superior outcomes compared to the response surface methodology [14].

A schematic representation of a hybrid clean energy setup is illustrated in **Figure 1**. This research constructs a model and simulates an integrated renewable energy framework incorporating solar PV, a wind turbine, a diesel-fueled generator, and consumer demand. An adaptive neuro-fuzzy inference system controller is established, and the entire configuration is evaluated from the perspective of energy generation and load distribution.

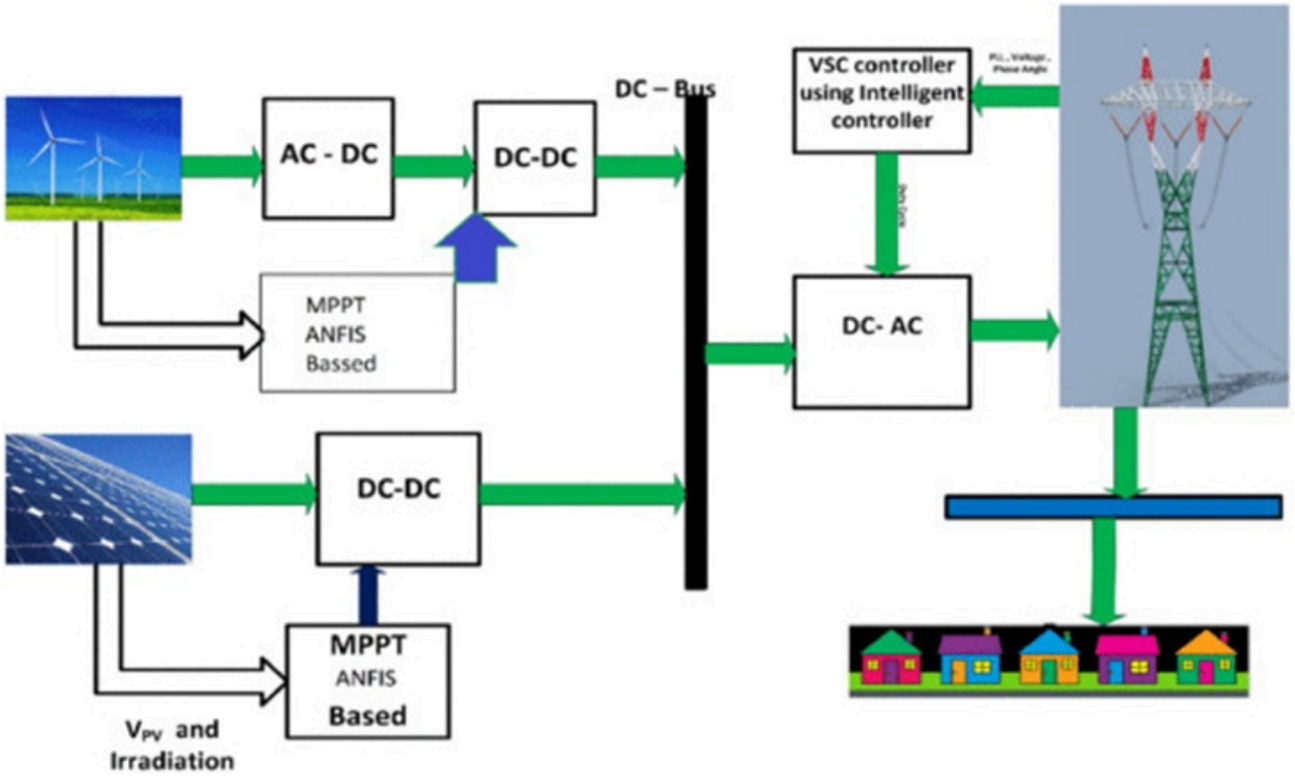


Figure 1. Diagram of a hybrid renewable energy system [15].

© 2024 The Author(s). | Published by Institute of Smart Energy Systems Press

The conceptual model depicted in **Figure 1** can evaluate the anticipated behavior of a solar generation framework relative to designated variables like solar irradiance, ambient temperature, and circuit resistance. Investigators have formulated diverse mathematical representations for PV equipment, with the single-diode model being the most fundamental. This approach strikes an appropriate balance between analytical simplicity and precision. Consequently, it is extensively implemented with both series and shunt resistances to illustrate how irradiance and temperature variations alter the PV module [16]. To establish appropriate integration with power electronics, optimized equations governing current (I) and voltage (V) in a single PV cell circuit, accounting for the influences of shunt and series resistance, must be derived [17].

Utilizing artificial neural networks (ANNs) within photovoltaic configurations has effectively managed power distribution and enhanced operational metrics [18]. By examining and forecasting disparate operational variables, including ambient solar irradiance and temperature, ANNs dynamically modify system outputs to meet electricity requirements [19]. A primary benefit of these control systems is their ability to adjust to fluctuating ambient conditions. Integrating ANN-centric regulation mechanisms into PV installations can markedly improve energy conversion ratios and overall reliability. The operational forecasting framework consists primarily of a collector mathematical formulation paired with an ANN predictive module. Typically, the transient fluid flow rate within the solar collector along with thermal parameters—encompassing input temperature, surrounding temperature, solar irradiance, and the thermal absorption surface area—serve as primary inputs for the collector's analytical model. The resulting fluid output temperature is commonly designated as an input parameter for the ANN. Maximum Power Point Tracking (MPPT) augments the generated power of PV setups to optimize energy capture efficacy.

Furthermore, voltage inverter metrics can be incorporated as inputs to refine MPPT execution by embedding the ANN as an internal black-box model. Solar radiation represents a highly viable form of clean power; nonetheless, its successful deployment is hindered by several constraints, particularly volatile weather trends. Investigators have adopted ANN strategies to minimize the adverse impacts of changing weather states on solar power management operations. ANNs can be trained to anticipate solar irradiance trends using retrospective datasets, thereby enhancing the efficiency of solar power capture infrastructure. The structural layout of this manuscript is organized as follows: the subsequent section outlines the photovoltaic (PV) power system.

Photovoltaic (PV) Energy System

The capacity of frameworks to anticipate power generation and load requirements facilitates superior optimization and operational efficiency. Using machine learning algorithms to analyze historical datasets and atmospheric trends enables accurate electricity output projections and dynamic operational parameter adjustments. Furthermore, AI-driven PV systems can track and respond to variations in electrical demand instantaneously, guaranteeing that power is utilized in an effective and economically viable manner. Broadly, integrating AI into energy oversight provides an encouraging strategy to elevate the sustainability and utility of PV installations. This structural stability has incentivized numerous clean energy firms to allocate resources toward this technology, leveraging it as a focal point for product advancement and commercial outreach. This progression is supported by an advanced engineering framework capable of disseminating this technological knowledge to local and regional territories. The effective deployment of renewable options is largely supported by the dominant temperate climate, which is highly favorable for the maximized performance of green power and PV setups. The mild annual mean temperatures and intense direct solar radiation observed in Jordan constitute critical prerequisites for maximizing PV operations. These environmental attributes have drawn global manufacturers to assess the efficiency of their PV hardware and perform validation tests to gather precise operational data regarding their novel designs. Autonomous PV installations are widely used in sectors lacking access to a centralized electrical grid [20]. An isolated PV configuration generally incorporates solar modules, an MPPT controller, a PID regulation unit, step-down (buck) and step-up (boost) power converters, alongside storage batteries [21]. Conversely, grid-tied setups are directly integrated with the commercial utility network, comprising solar panels, one or multiple power inverters, a main distribution board, electrical loads, a metering unit, and the central grid infrastructure. A solar photovoltaic (SPV) cell directly converts incoming sunlight into electrical power. This electricity corresponds to a directed movement of electrons.

© 2024 The Author(s). | Published by Institute of Smart Energy Systems Press

Fundamentally, external energy inputs are necessary to detach electrons from their atomic nuclei. Within an atom, valence electrons occupy the highest energy states while remaining bound to their host structure. Extricating an electron requires supplementary energy, meaning that unbonded or free electrons exhibit higher energy states relative to valence electrons. A full PV array is fabricated by interconnecting multiple modules in both series and parallel topologies. The resulting PV array operates as a non-linear network defined by its equivalent electrical circuit configuration alongside its characteristic P(V) and I(V) relationships [11], as illustrated in **Figure 2.**

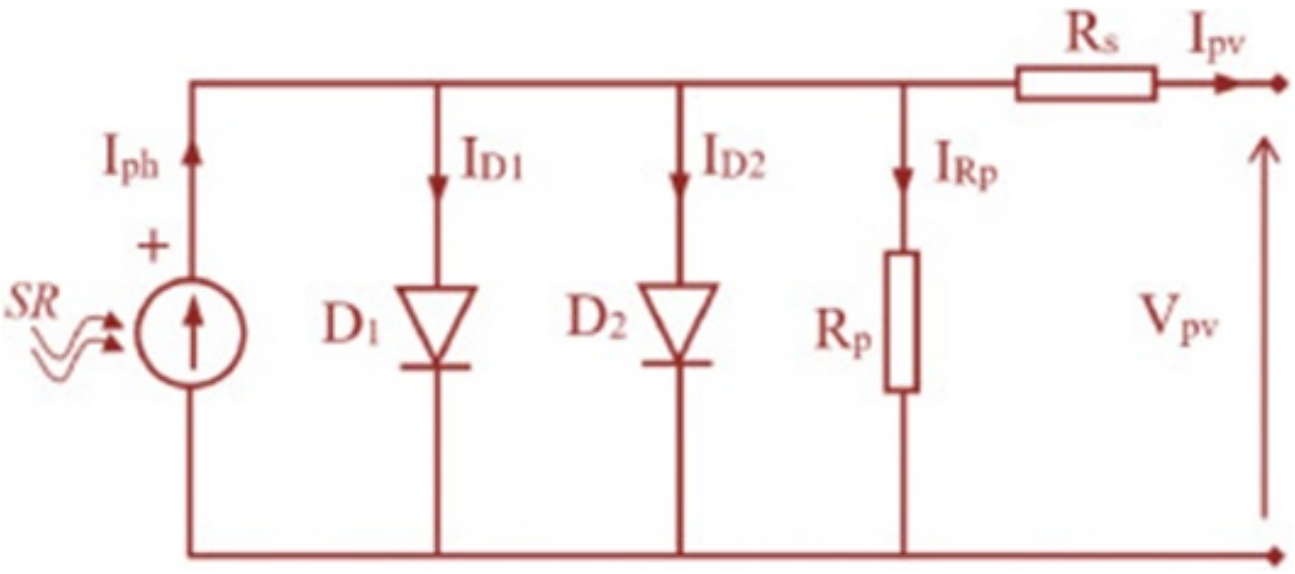


Figure 2. Equivalent electrical circuit for PV solar cell.

Diverse analytical models have been formulated to capture the semiconductor junction relationships governing this non-linear performance, with the 'Four-Parameter Model' being the most frequently utilized. The operational efficiency of monocrystalline and polycrystalline PV arrays has been comprehensively analyzed in Ammar *et al*. [22].

The current of the equivalent circuit Ipv can be expressed based on the voltage of the PV array Vpv, in the following manner [11]:

$$I_{pv} = I_{sc}\left\{1 - F_{11}\left[exp\left(F_{22}V_{pv}^{m}\right) - 1\right]\right\} \quad (1)$$

Where:

$$F_{11} = 0.01175 \quad (2)$$

$$F_{22} = F_{44}/V_{oc}^{m} \quad (3)$$

$$F_{33} = ln\left[\frac{I_{sc}(1 + F_{11}) - I_{mpp}}{F_{11}I_{sc}}\right] \quad (4)$$

$$F_{44} = ln\left[\frac{1 + F_{11}}{F_{11}}\right] \quad (5)$$

Where Vmpp represents the MPP voltage, and Impp signifies the MPP current. The designation OC represents the open-circuit voltage (Voc), while SC reflects the short-circuit current (Isc).

© 2024 The Author(s). | Published by Institute of Smart Energy Systems Press

The performance of the PV setup is typically influenced by meteorological factors, specifically ambient temperature and solar irradiance. To solve **Eq. 1**, the following expressions are applicable.

$$T_c = T_a + (NOCT - T_0)\frac{G}{G_0} \quad (7)$$

$$\Delta T_C = T_C - T_0 \quad (8)$$

$$\Delta I_{pv} = \alpha \frac{G}{G_0}\Delta T_C + \left(\frac{G}{G_0} - 1\right) I_{sc} \quad (9)$$

$$\Delta V_{pv} = -\beta\ \Delta T_C - R_s\ \ \Delta I_{pv} = \frac{ln[F_{33}/F_{44}]}{ln[V_{mpp}/V_{oc}]} \quad (10)$$

T0 represents the solar cell temperature, and G0 denotes the solar irradiance under standard test conditions. Tc corresponds to the temperature of the solar cell, G indicates the operational irradiance, and Ta signifies the surrounding ambient temperature. The parameter A stands for the SCC temperature coefficient, whereas β represents the OCV temperature coefficient. The variable Rs denotes the series resistance.

The updated PV current parameter is given by **Eq. 11**, and the updated PV voltage parameter is defined by **Eq. 12:**

$$V_{pv,new} = V_{pv} + \Delta V_{pv} \quad (11)$$

$$I_{pv,new} = I_{pv} + \Delta I_{pv} \quad (12)$$

The corresponding PV power output can be calculated via **Eq. 13** [20, 21].

$$P_{pv} = N_{SS} V_{pv}\ N_{PP}\ I_{pv} \quad (13)$$

In this context, NSS reflects the series connection of the PV cells, and NPP indicates the parallel connection of the PV cells.

The operational parameters of the API-M255 PV solar panel are detailed in **Table 1.**

Table 1. The PV module characteristics.

Advanced power API-M255	
P_{max}	255.51 W
V_{mpp}	30.6 V
I_{mpp}	8.35 A
V_{oc}	37.68 V
I_{sc}	8.67 A

© 2024 The Author(s). | Published by Institute of Smart Energy Systems Press

R_S	0.3004 Ω
R_P	1773. 68 Ω
N_{cell}	60

Maximum Power Point Tracking (MPPT) Technique Description

Multiple strategies exist for tracking the maximum power point (MPP). These approaches include the incremental conductance method, the fractional OCV scheme, the fractional SCC strategy, artificial neural network methods, and fuzzy logic control [23].

In this investigation, a fuzzy logic controller (FLC) was selected as the designated MPPT approach. The FLC framework governs the PV system utilizing a knowledge-based data methodology. The essential phases of the FLC are depicted in **Figure 3.**



Figure 3. The Block diagram for the FLC technique.

The FLC input variables ER and the corresponding FLC output CEr are established as follows:

$$\begin{cases} E_r = \dfrac{P_{pv}(K) - P_{pv}(K-1)}{V_{pv}(K) - V_{pv}(K-1)} \\ CE_r = E(K) - E(K-1) \end{cases} \quad (14)$$

Where K represents the sampling interval. The membership functions (MFs) governing the FLC inputs Er, the FLC output CEr, and the operating duty cycle (D) are presented in **Figure 4**. Every MF incorporates five distinct fuzzy sets: NN, PN, ZR, NP, and PP (in which N and P denote low and high values, respectively). The matrix of operational rules is detailed in **Table 2**.

© 2024 The Author(s). | Published by Institute of Smart Energy Systems Press

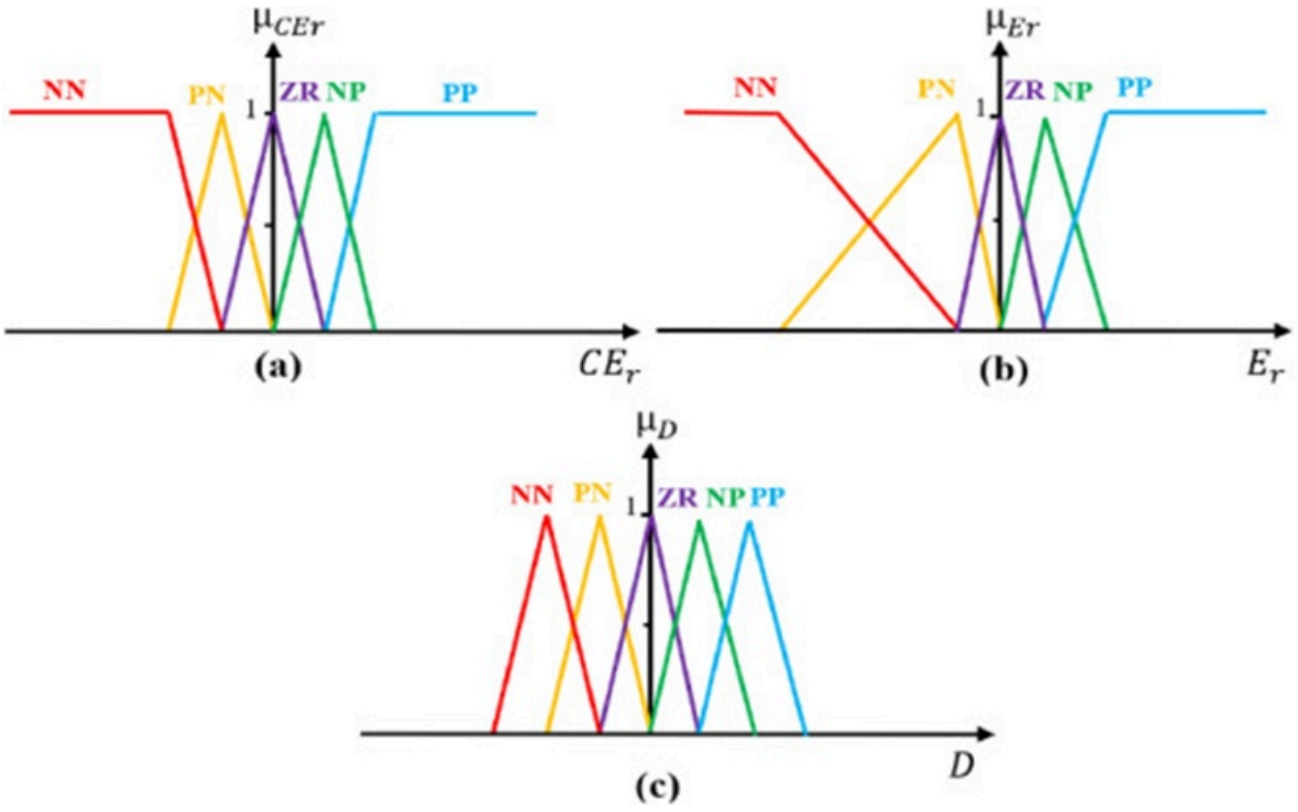


Figure 4. Input and output MFs. Legends: (a): μCEr, (b): μEr and (c): μD.

Table 2. Fuzzy rules.

CE_r	E_r				
	NN	**PN**	**ZR**	**NP**	**PP**
NN	PP	PP	NP	PP	PP
PN	PP	NP	NP	NP	PP
ZR	PN	PN	ZR	NP	NP
NP	NN	PN	PN	PN	NN
PP	NN	NN	PN	NN	NN

Membership functions (MFs) define the degree of fuzziness inherent to fuzzy sets. Due to their linear nature and computational simplicity, triangular MFs are heavily utilized. They deliver high performance, frequently surpassing alternative MF profiles. Different geometric distributions can be derived by modifying the basic triangle through linguistic modifiers, truth-functional adjustments, compositions, projections and other analytical operations [23].

Boost converter modeling

Modeling the boost converter is essential for the precise prediction of PV system efficiency. This converter circuit modifies the direct current (DC) voltage generated by the PV panels to align with the electrical demands of the grid or load. This process profoundly influences the system's overall efficacy. Analytical models detailing the operational dynamics of the

© 2024 The Author(s). | Published by Institute of Smart Energy Systems Press

boost converter can be formulated by factoring in diverse variables, including the control strategy, switching frequency, and converter topology. Such models can simulate converter operation and refine the architecture, ultimately enhancing the operational performance of the PV network.

$V_{out} = \frac{V_{in}}{1-D}$ (1) Where D represents the duty cycle.

The electrical circuit depicted in **Figure 5** is realized using Simulink, as illustrated in **Figure 6.**

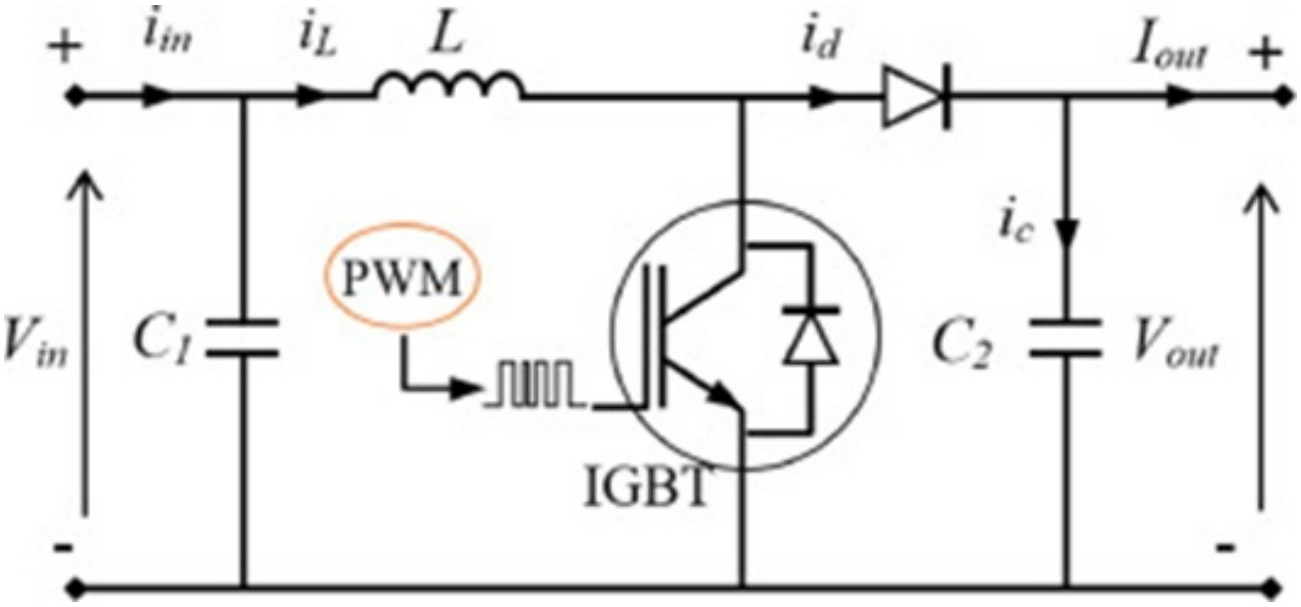


Figure 5. The circuit model of the DC/DC boost converter.

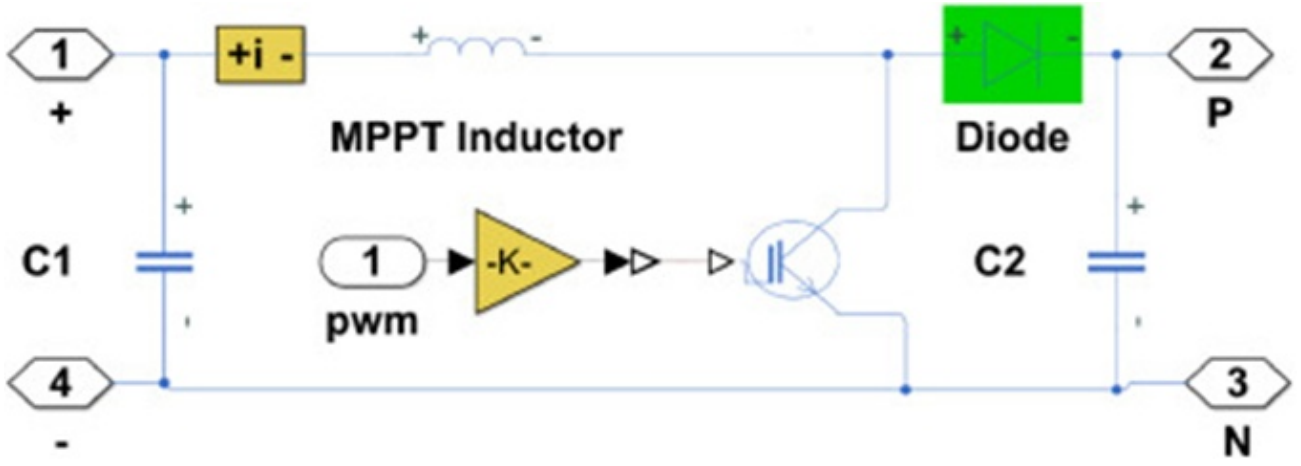


Figure 6. Simulink implementation of the DC/DC converter.

The dual operational states of the converter—specifically, passing and blocking—are delineated in the subsequent equations [24].

$$\frac{di_L}{dt} = \frac{1}{L}[V_{in} - V_{out}(1-D)] \quad (16)$$

© 2024 The Author(s). | Published by Institute of Smart Energy Systems Press

$$\frac{dV_{out}}{dt} = \frac{1}{C_1}[i_L(1-D) - I_{out}] \quad (17)$$

L denotes the inductance, the current through the inductor, C1 represents the input capacitance, and Iout signifies the current of the load.

Lithium-Ion battery bank modeling

The representation of the lithium-ion battery is depicted in **Figure 7**. MATLAB/Simulink was utilized for this modeling. Furthermore, the circuit's realization via Simulink is presented in **Figure 8**.

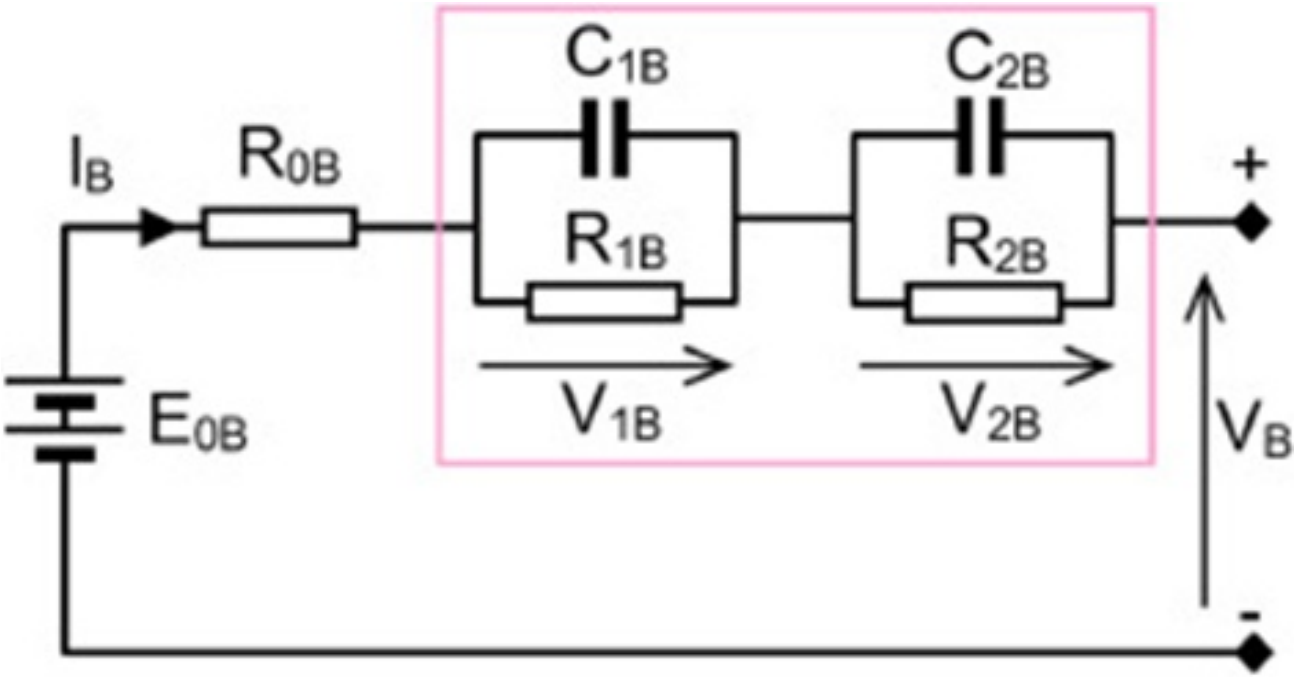


Figure 7. Lithium-ion battery model.

© 2024 The Author(s). | Published by Institute of Smart Energy Systems Press

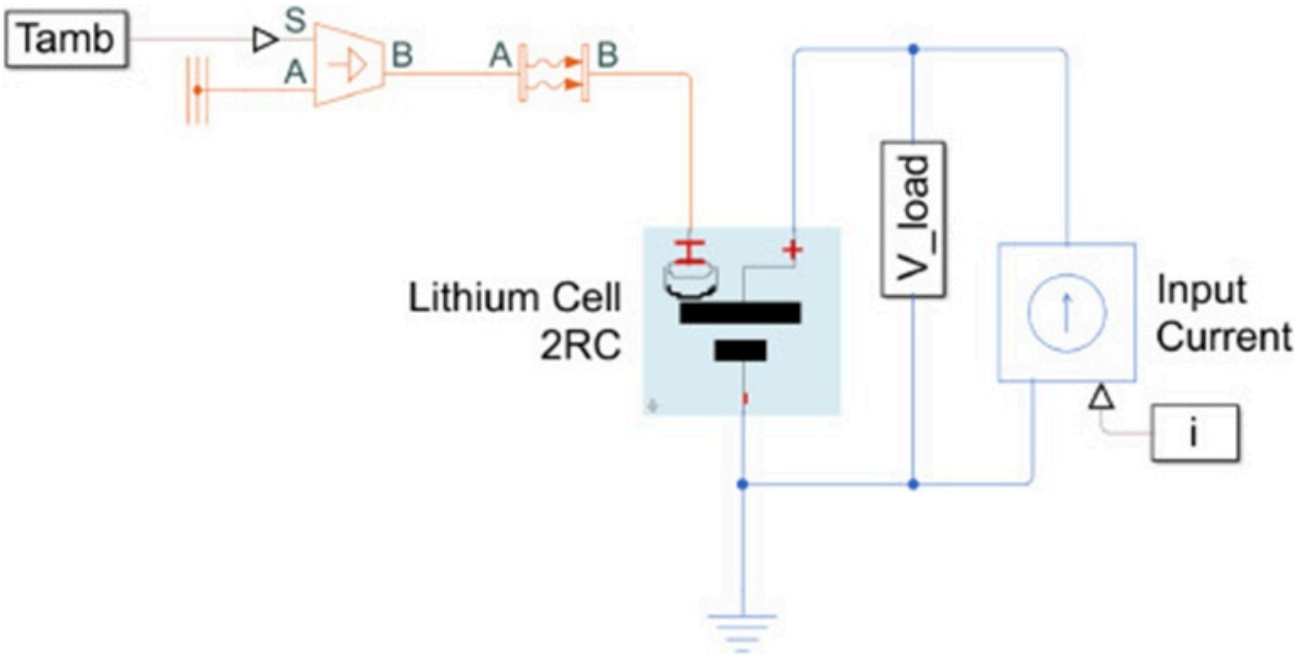


Figure 8. Simscape Lithium-ion battery model.

This approach is applied to minimize computational demands and address flaws in the obsolete Equivalent Circuit Model (ECM), thereby sustaining a superior trajectory across ECMs. The state of charge (SOC) of the battery measures the available energy during the current cycle,

$$SOC(t) = SOC(t0) - \frac{\int_{t0}^{t} I_B(\tau)d\tau}{Q_C} \quad (18)$$

In this context, IB represents the current, QC denotes the rated capacity, and t0 indicates the starting time. To calculate the SOC, the Coulomb counting technique was employed by assessing the measured discharge current and performing time integration. By differentiating **Eq. 18** with respect to t, the following is yielded:

$$\dot{SOC}(t) = -\frac{I_B(t)}{Q_C} \quad (19)$$

Utilizing the schematic in **Figure 7**, the determination of voltage VB is executed as follows:

$$V_B(t) = E_0(SOC) - I_B(t)R - C(t) \quad (20)$$

R denotes the internal resistance, whereas C(t) acts as an adjustment factor compensating for environmental variations and model imprecision [23]. Within this framework, an ECM configuration featuring a 2-RC circuit is implemented:

$$\dot{V_1}(t) = -\frac{V_{1B}(t)}{R_{1B}C_{1B}} + \frac{I_B(t)}{C_{1B}} \quad (21)$$

$$\dot{V_2}(t) = -\frac{V_{2B}(t)}{R_{2B}C_{2B}} + \frac{I_B(t)}{C_{2B}} \quad (22)$$

© 2024 The Author(s). | Published by Institute of Smart Energy Systems Press

R1B alongside R2B act as the diffusion resistances of the RC network, while C1B and C2B constitute the diffusion capacitances.

The corresponding Simulink model for the PID controller is illustrated in **Figure 9.** This configuration incorporates two switching mechanisms. The Sp1 switch facilitates battery charging, whereas the Sn1 switch manages the discharging phase.

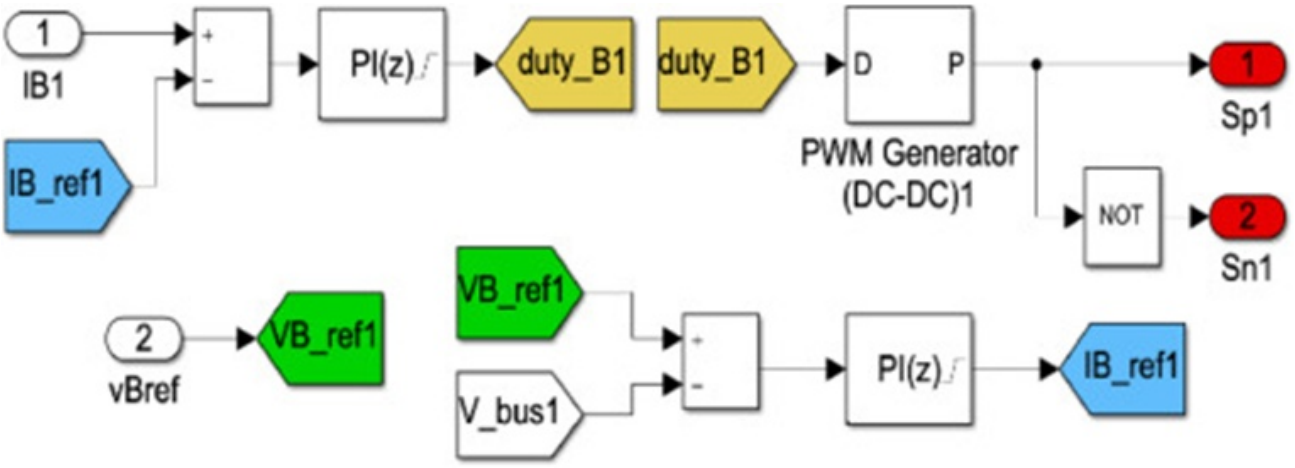


Figure 9. Discrete PID controller Simulink model.

Forecasting PV performance

The incorporation of renewable power sources into building infrastructures and electrical grids is imperative for promoting sustainable energy consumption. Consequently, PV frameworks have gained widespread traction owing to their demonstrated capability to produce electrical power from solar irradiance. Nevertheless, the fluctuating characteristics of solar power must be managed to ensure efficient use of the generated energy; this necessitates PV performance forecasting. By formulating precise estimations of power yield, configurations can be engineered to accommodate variability, ensuring a more consistent and dependable energy supply.

Utilizing the ANN ToolBox in MATLAB, regression algorithms were developed for both battery SOC and solar power output, incorporating daily measured input variables. Real-time operational metrics—including input currents, solar array parameters, and power generation—are recorded hourly. This information serves as training material to predict solar energy yield at 30-minute increments for the current day. Subsequently, these 30-minute projections are employed to forecast the solar energy production for the successive day. For this investigation, a feed-forward neural network framework was considered.

The SOC of the battery is determined by processing real-time operational metrics, specifically solar generation and battery charging currents, which act as target input signals. To project the battery SOC for the next day, empirical data collected at hourly intervals are integrated with projected values generated at 30-minute steps. Throughout this methodology, the electrical load connected to the network remains unvarying.

Artificial Neural Network Basic Controller Design

Managing energy within PV installations is a critical concern in renewable energy research. Deploying an artificial neural network (ANN) is one viable strategy for regulating this mechanism. ANN-based controllers are increasingly favored

© 2024 The Author(s). | Published by Institute of Smart Energy Systems Press

because they can adapt to diverse conditions and improve energy conversion efficiency.

Formulating a fundamental ANN controller requires understanding its inherent properties, selecting suitable input and output variables, and refining the network's architecture. In recent times, ANN methodologies have drawn attention for their ability to represent fuzzy inference mechanisms using neural training functions. This architecture comprises distinct nodes performing specialized tasks, organized into sequential layers, as depicted in **Figure 10.**

A fuzzy logic system can be systematically trained and calibrated using a neuro-fuzzy inference framework. During this training phase, membership functions (MFs) are optimized using the provided input and output datasets [24].

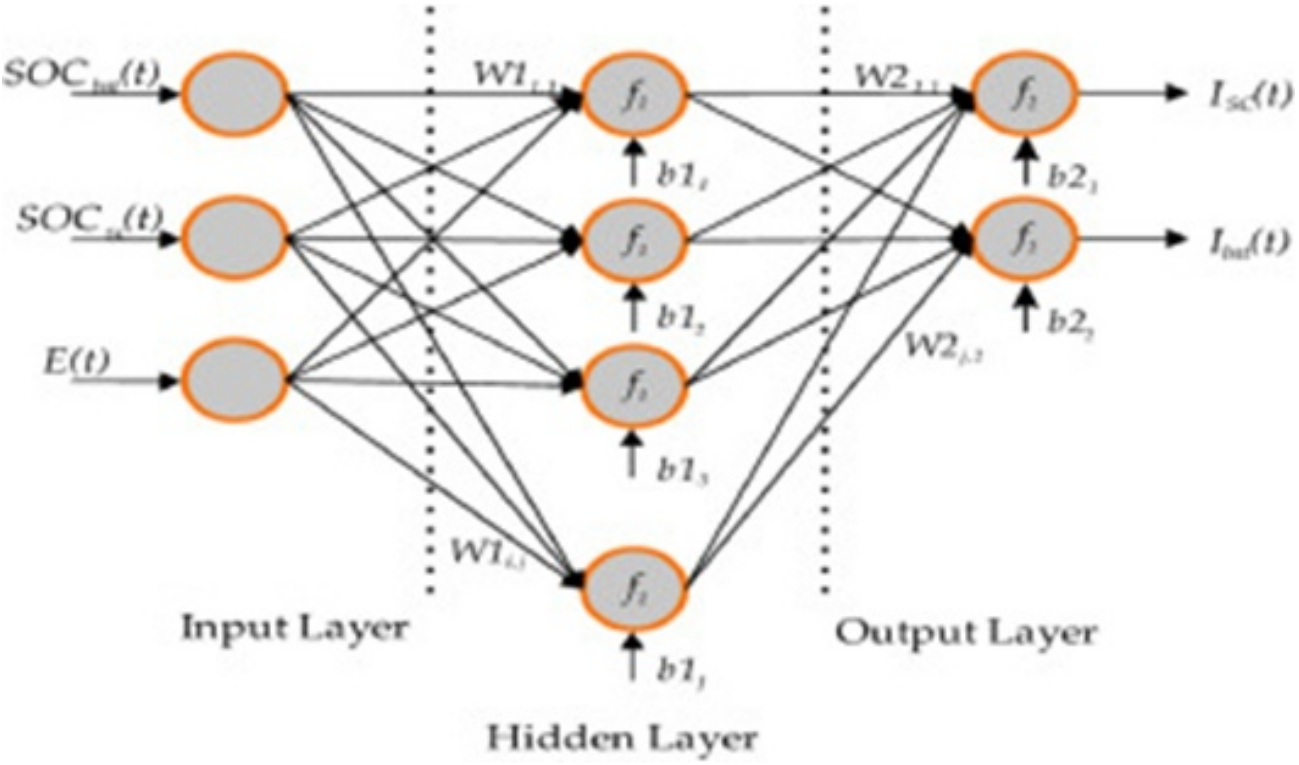


Figure 10. Multi-layer feed-forward neural network architecture.

To guarantee compliance with manufacturer guidelines, the ANN is programmed to govern the charging and discharging protocols relative to the rated capacity of the lithium-ion battery banks. To mitigate peak currents and alleviate dynamic strain on the lithium-ion cells, the allowable discharge current was established. These operational thresholds were chosen in accordance with specific percentage fractions of the batteries' nominal capacities.

An illustrative diagram of the proposed AI-driven control architecture for PV energy management is presented in **Figure 11**. The core components of this electrical framework include a photovoltaic (PV) generation unit, a battery management system (BMS), a boost converter, and an alternating current (AC) load integrated with a neuro-fuzzy regulator. To ensure operation at peak capacity regardless of thermal conditions or solar irradiance variations, the solar modules interface directly with a maximum power point tracker (MPPT). The BMS is tasked with monitoring the battery array's DC voltage and temperature. By continuously evaluating the SOC, the remaining stored energy is strictly observed. Consequently, the BMS prevents anomalous battery degradation caused by detrimental charging behaviors, excessive discharging, overcharging, or abnormal thermal states. Furthermore, the boost converter serves as the critical link uniting the PV array, the battery energy storage system (BESS), and the ANFIS regulatory setup. This integration enables the boost converter to identify system faults while leveraging data tracked during the neural network's validation and training phases to

© 2024 The Author(s). | Published by Institute of Smart Energy Systems Press

contrast the provisional load against the production profile and select the optimal tactic for minimizing peak consumption events [24].

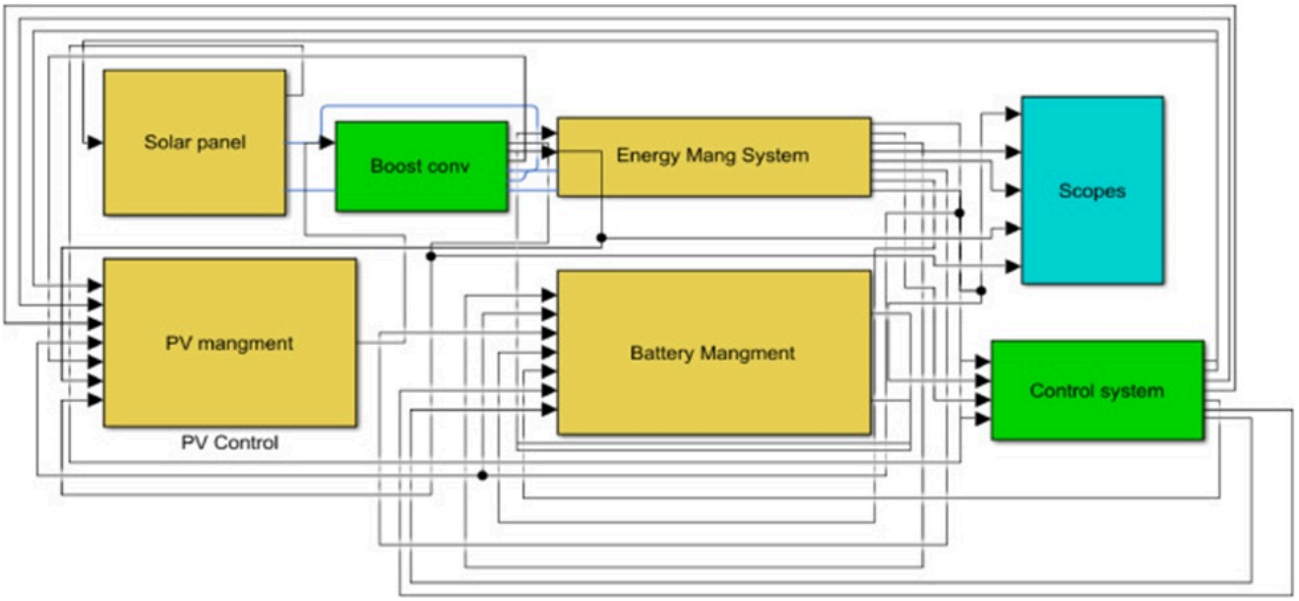


Figure 11. Simulink implementation of the proposed system.

The architectural fusion of Sugeno-style fuzzy logic with artificial neural networks (ANN) yields what is termed an Adaptive Neuro-Fuzzy Inference System (ANFIS). To refine fuzzy logic rules and membership functions, the ANFIS framework utilizes an ANN methodology known as backpropagation. **Table 3** lists the various research domains that may be investigated when sizing a standalone PV network using ANN.

Table 3. Applications of ANN in PV systems.

PV sizing method	ANN research area
Load assessment	ANN can be employed to estimate the total electrical demand of a building or residence. Inputs may include information such as appliance categories, power ratings, geographical location, and weather conditions.
Determination of the required number of solar panels	ANN can be utilized to forecast the number of PV modules required. The ANN inputs may be modified as needed, and the mathematical expression used for PV panel sizing can serve as an input variable. Different ANN architectures can be implemented and evaluated.
Battery bank sizing calculation	ANN can be applied to predict the required battery bank capacity. Input parameters can be adjusted, and the battery-sizing formula may be incorporated as an input feature. Various ANN structures can be tested and compared.
Sizing of additional components, including the inverter and solar charge controller	ANN can be used to estimate the appropriate sizes of the inverter and solar charge controller. The ANN input set can be customized, and multiple ANN configurations can be developed and assessed for performance.

© 2024 The Author(s). | Published by Institute of Smart Energy Systems Press

Results and Discussion

The theoretical discharge profiles of dual series-linked 200Ah, 12 V, and 10C lead-acid battery units subjected to loads of 400 W, 500 W, and 600 W (corresponding to 16.667A, 20.833A, and 25A, respectively) are illustrated in **Figure 12**. These measurements were recorded within a real-time operational environment. Whenever the state of charge (SOC) surpasses 70% and the voltage drops by approximately 20 V, the inverter extracts power from the utility grid to replenish the battery's SOC to 100%. The forecasted simulation data extend down to a voltage level of zero. Under such operational parameters, the voltage data available for training the artificial neural network (ANN) are limited to a maximum of 20 V. Furthermore, the rate at which the voltage decreases is a critical factor when dealing with a low initial SOC under heavy load conditions.

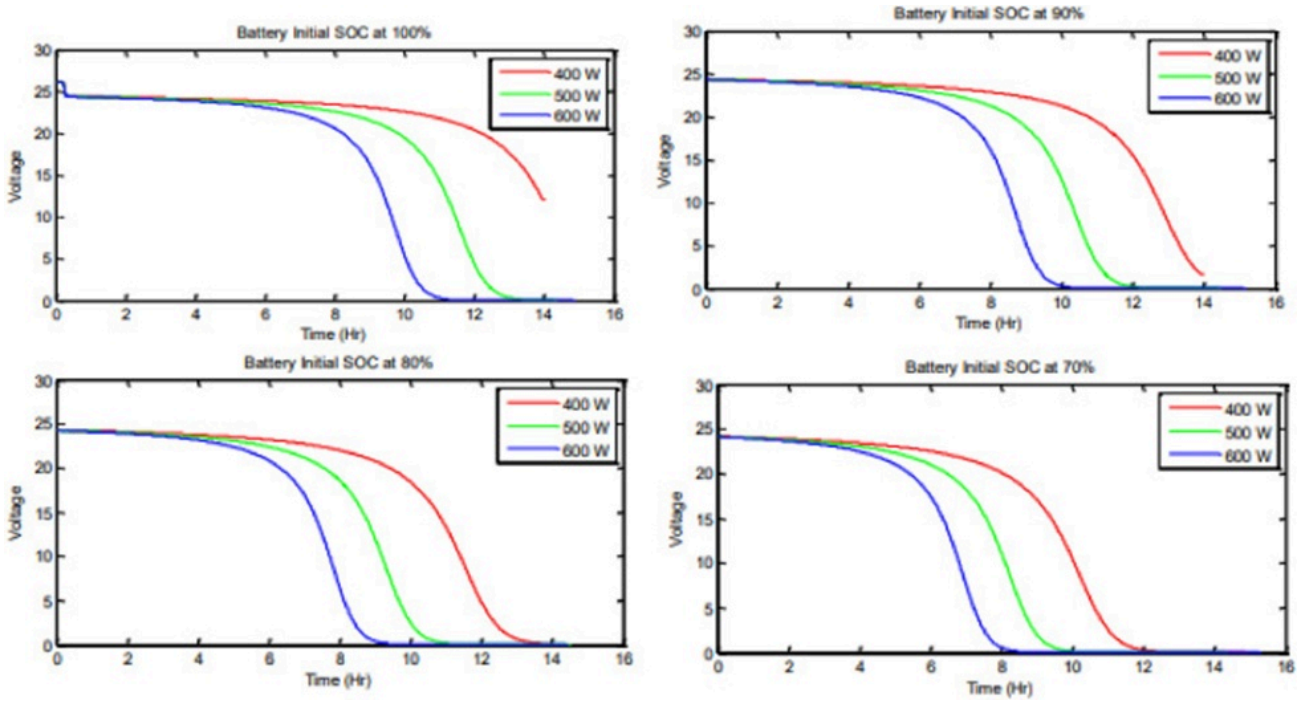
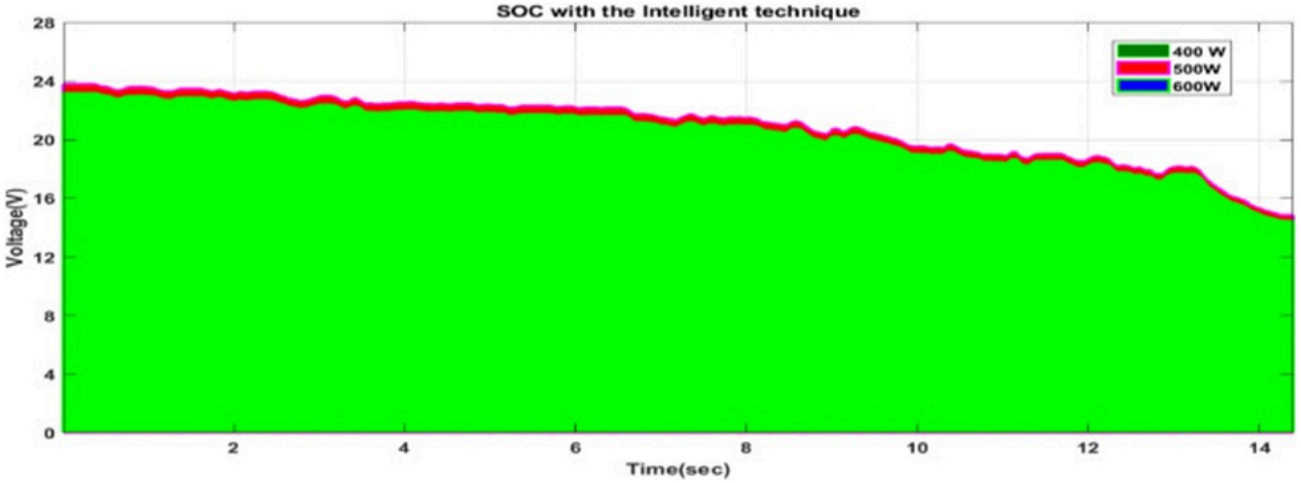


Figure 12. Battery discharge characteristics for various initial SOC loads.

As depicted in **Figure 13**, managing the SOC through the proposed intelligent methodology guarantees highly stable and seamless performance across various power ranges and extended operational durations, demonstrating superiority over conventional approaches.



© 2024 The Author(s). | Published by Institute of Smart Energy Systems Press

Figure 13. SOC behavior using intelligent technique.

Figure 14 illustrates the efficiency of the solar PV system alongside the charging states. The system achieves an efficiency rate of 91%, characterized by highly stable and consistent operation. Furthermore, the phase and magnitude of the various system parameters are presented in **Figure 15,** which similarly reflects steady operational behavior. The modulation of the 2RC battery model using the adaptive neuro-fuzzy inference system (ANFIS) is detailed in **Figure 16**. Additionally, the specific parameters concerning the ANFIS setup are summarized in **Table 4.**

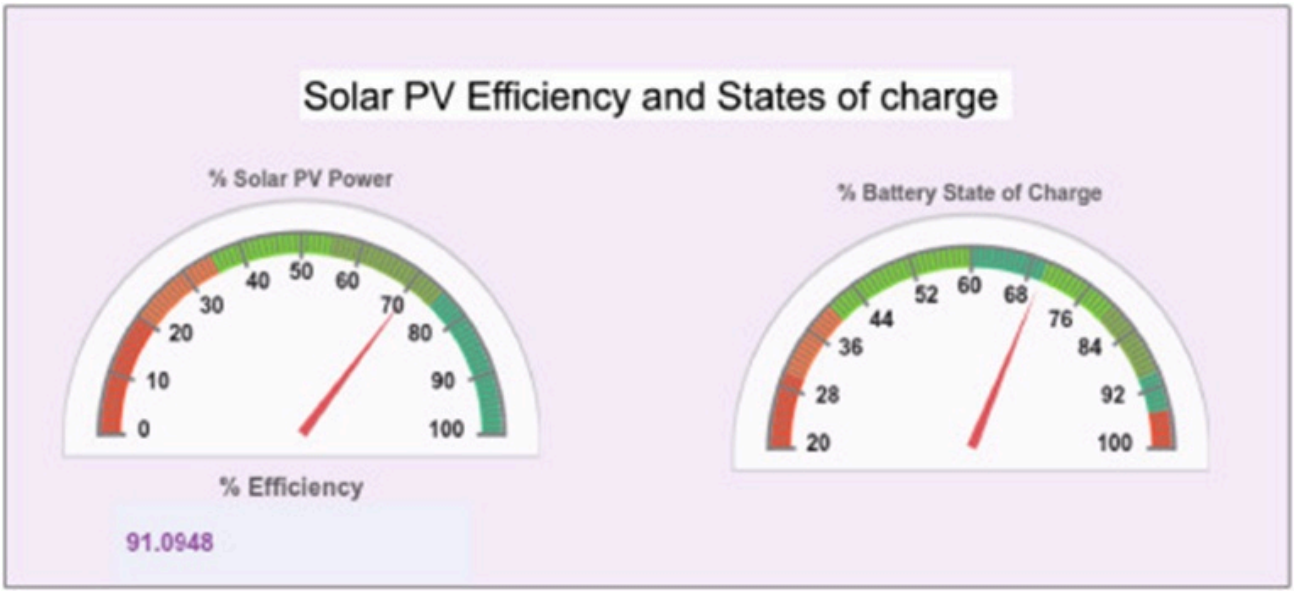


Figure 14. Solar PV efficiency and state of charge.

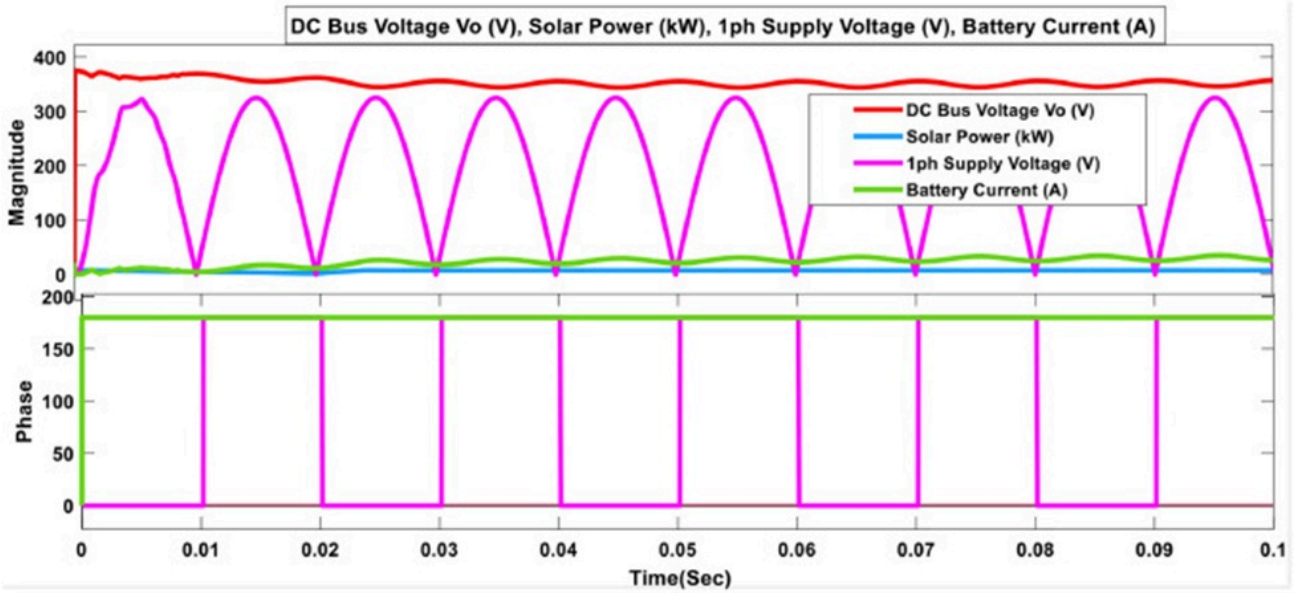


Figure 15. System parameters magnitude and phase.

© 2024 The Author(s). | Published by Institute of Smart Energy Systems Press

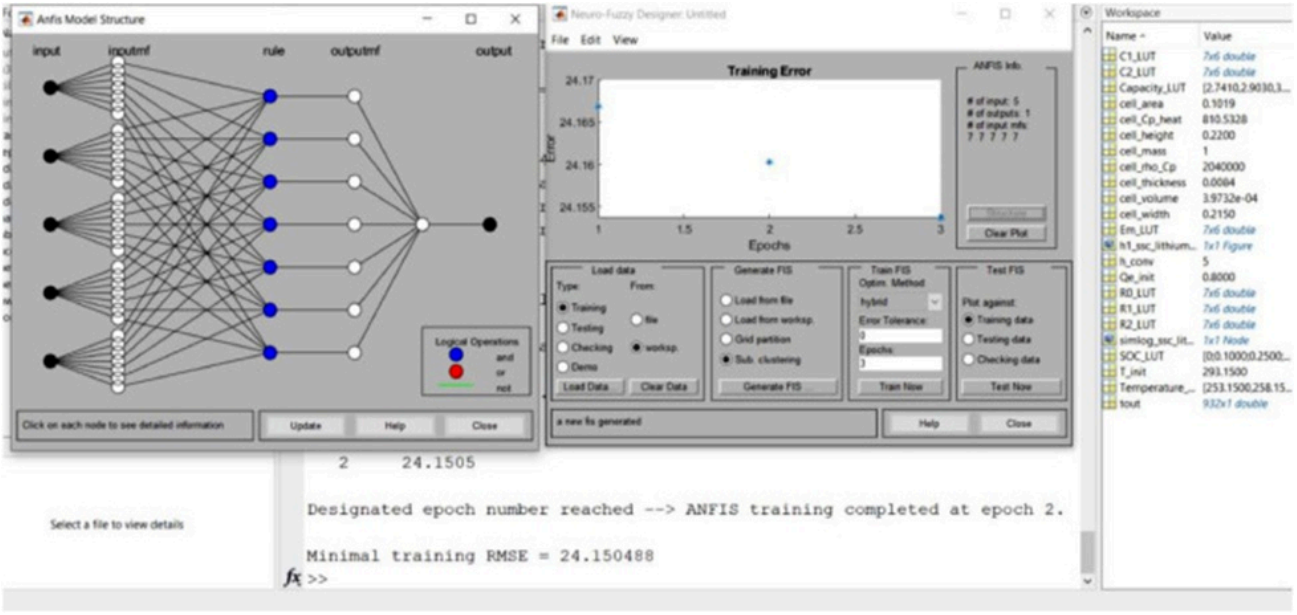


Figure 16. ANFIS structure and training error of the battery.

Table 4. ANFIS information.

Parameter	Value
Number of nodes	92
Number of linear parameters	42
Number of non-linear parameters	70
Total number of parameters	112
Number of training data pairs	7
Number of checking data pairs	0
Number of fuzzy rules	7
ANFIS Training Start	1 → 1.07058e-07 2 → 1.07092e-07

Conclusion

The increasing integration of photovoltaic (PV) facilities into the power grid is largely driven by the availability of geographically optimal locations for solar deployment. The approach presented in this study enables the calculation of essential battery capacities and PV array dimensions using geographical coordinates, which is especially valuable for remote areas where comprehensive global solar irradiance data are unavailable. Additionally, this technique can be utilized to evaluate the operational efficiency of commercial PV installations and model the enhancement of direct current (DC) to alternating current (AC) inverters. The results reveal a significant correlation between output current and voltage between a PV converter and a transducer functioning under a steady DC input. Historically, PV architectures have delivered substantial benefits to multiple consumer demographics, reflecting a steady expansion in their market penetration over time.

© 2024 The Author(s). | Published by Institute of Smart Energy Systems Press

Furthermore, the volatility of electricity prices plays a crucial role in directing the future expansion trajectory of PV infrastructure. The introduced battery management system (BMS), augmented by artificial intelligence (AI) techniques, demonstrated high efficiency across all levels of battery discharge. Integrating this control mechanism within the energy management unit enhanced overall system functionality, ensuring that stored energy adequately meets load demands. Ultimately, the Adaptive Neuro-Fuzzy Inference System (ANFIS) proves to be a robust methodology for designing and assessing PV energy management frameworks. Despite these advancements, the widespread adoption of PV systems still faces significant barriers, such as a lack of strategic foresight, limited public awareness of the benefits of solar energy, and protracted grid interconnection processes. For this study, a PV-driven DC-DC boost converter was developed and applied to regulate exposure levels while preserving thermal stability. This novel configuration clearly demonstrated exceptional performance, highlighting its perceived superiority in managing energy transfer across dual PV installations.

Acknowledgements

None

Conflict of interest

None

Financial support

None

Ethics statement

None

Received: 06 Feb 2023 Revised: 13 Apr 2023 Accepted: 28 Apr 2023
Published online: 15 November 2024

Rights and permissions

Open Access The author(s) retain copyright. This article is licensed under the Creative Commons Attribution-NonCommercial-ShareAlike 4.0 International License. It may be shared and adapted for non-commercial purposes with appropriate attribution, an indication of changes, and distribution of adaptations under the same license. Third-party material may be subject to separate terms identified in its credit line. View the license at https://creativecommons.org/licenses/by-nc-sa/4.0/.

References

1. Gaeid KS, Al Smadi T, Abubakar U. Double control strategy of PMSM rotor speed-based traction drive using resolver. Results Control Optim. 2023;13:100301. https://doi.org/10.1016/j.rico.2023.100301.

2. Svazas M, Navickas V, Bilan Y, Vasa L. The features of the shadow economy impact' on the biomass energy sector. Energies. 2022;15:2932.

3. Handam A, Al Smadi T. Multivariate analysis of efficiency of energy complexes based on renewable energy sources in the system power supply of autonomous consumer. Int J Adv Appl Sci. 2022;9(5):109-18. https://doi.org/10.21833/ijaas.2022.05.014.

4. Zapar WM, Gaeid K, Mokhlis HBM, Al Smadi TA. Review of the most recent articles in fault tolerant control of power plants 2018–2022. Tikrit J Eng Sci. 2023 Jul;30(2):103-13. https://doi.org/10.25130/tjes.30.2.11.

5. Gaeid KS, Homod RZ, Mashhadany YA, Smadi TA, Ahmed MS, Abbas AE, et al. Describing function approach with PID controller to reduce nonlinear action. Int J Electr Electron Res. 2022;10(4):976-83. https://doi.org/10.37391/ijeer.100437.

6. Zhou Y. Sustainable energy sharing districts with electrochemical battery degradation in design, planning, operation and multi-objective optimization. Renew Energy. 2023;202:1324-41. https://doi.org/10.1016/j.renene.2022.12.026.

7. Al-Husban Y, Al-Ghriybah M, Handam A, Al Smadi T, Al Awadi R. Residential solar energy storage system: state of the art, recent applications, trends, and DEVELOPME. J Southwest Jiaotong Univ. 2022;57(5):750-69. https://doi.org/10.35741/issn.0258-2724.57.5.61.

8. Trrad I, Smadi TA, Al_Wahshat H. Application of fuzzy logic to cognitive wireless communications. Int J Recent Technol Eng. 2019;8(3):2228-34.

9. Ravada BR, Tummuru NR, Ande BNL. Photovoltaic-wind and hybrid energy storage integrated multisource converter configuration-based grid-interactive microgrid. IEEE Trans Ind Electron. 2020;68:4004-13.

10. Boussetta M, Motahhir S, El Bachtiri R, Allouhi A, Khanfara M, Chaibi Y. Design and embedded implementation of a power management controller for wind-PV-diesel microgrid system. Int J Photoenergy. 2019;2019:16 pages.

11. Alzaroog E, Ammar MB, Zdiri MA, Abdallah HH. An advanced artificial neural network energy management in standalone PV systems. Int J Electr Electron Res. 2022;10(4):1005-12.

12. Jiménez-Castillo G, Muñoz-Rodríguez FJ, Rus-Casas C, Hernández JC, Tina GM. Monitoring PWM signals in stand-alone photovoltaic systems. Measurement. 2019;134:412-25.

13. Sugiarti Y, Na'am J, Indra D, Santony J. An artificial neural network approach for detecting skin cancer. TELKOMNIKA (Telecommun Comput Electron Control). 2019;17(2):788-93.

14. Arun P. Sizing curve for isolated photovoltaic-battery systems using artificial neural networks. In: 2nd International Conference on Green Energy and Applications (ICGEA). 2018. p. 147-51.

15. Kumar Vankadara S, Chatterjee S, Balachandran PK. Applications of metaheuristic algorithms for MPPT under partial shaded condition in PV system. In: 2023 4th International Conference for Emerging Technology (INCET). 2023 May. https://doi.org/10.1109/incet57972.2023.10170183.

16. Takialddin AS, Al-Agha OI, Alsmadi KA. Overview of model free adaptive (MFA) control technology. IAES Int J Artif Intell. 2018;7(4):165. https://doi.org/10.11591/ijai.v7.i4.pp165-169.

17. Vankadara SK, Chatterjee S, Balachandran PK. An accurate analytical modeling of solar photovoltaic system considering Rs and Rsh under partial shaded condition. Int J Syst Assur Eng Manag. 2022;13(5):2472-81. https://doi.org/10.1007/s13198-022-01658-6.

18. Aljafari B, Balachandran PK, Samithas D, Thanikanti SB. Solar photovoltaic converter controller using opposition-based reinforcement learning with butterfly optimization algorithm under partial shading conditions. Environ Sci Pollut Res.

© 2024 The Author(s). | Published by Institute of Smart Energy Systems Press

2023;30(28):72617-40.
https://doi.org/10.1007/s11356-023-27261-1.

19. Al-Husban Y, Al-Ghriybah M, Gaeid KS, Takialddin AS, Handam A, Alkhazaleh AH, et al. Optimization of the residential solar energy consumption using the taguchi technique and box-behnken design: a case study for jordan. Int J Energy Conver. 2023;11(1):25.
https://doi.org/10.15866/irecon.v11i1.22672.

20. Wali SA, Muhammed AA. Power sharing and frequency control in inverter-based microgrids. Tikrit J Eng Sci. 2022;29(3):70-81.

21. Ammar RB, Ammar MB, Oualha A. Photovoltaic power forecast using empirical models and artificial intelligence approaches for water pumping systems. Renew Energy. 2020;153:1016-28.

22. Ammar MB, Ammar RB, Oualha A. Photovoltaic power prediction for solar car park lighting office energy management. J Energy Resour Technol. 2020;143(3):1-11.

23. Zdiri MA, Ben Ammar M, Bouzidi B, Abdelhamid R, Abdallah HH. An advanced switch failure diagnosis method and fault tolerant strategy in photovoltaic boost converter. Electr Power Compon Syst. 2020;48(18):1932-44.

24. Ammar MB, Zdiri MA, Ammar RB. Fuzzy logic energy management between stand-alone PV systems. Int J Renew Energy Res. 2021;11(3):1238-49.

© 2024 The Author(s). | Published by Institute of Smart Energy Systems Press